

# Influence of the Electrostatic Interactions on the Thermophysical Properties of Polyimides: Molecular-Dynamics Simulations

Stanislav G. Falkovich,<sup>1</sup> Sergey V. Lyulin,<sup>1,2</sup> Victor M. Nazarychev,<sup>1</sup> Sergey V. Larin,<sup>1</sup> Andrey A. Gurtovenko,<sup>1,2</sup> Natalia V. Lukasheva,<sup>1</sup> Alexey V. Lyulin<sup>3</sup>

<sup>1</sup>Institute of Macromolecular Compounds, 31, Bolshoi pr., Saint-Petersburg 199004, Russia

<sup>2</sup>Department of Physics, St. Petersburg State University, Ulyanovskaya Str. 1, Petrodvorets, St, Petersburg 198504, Russia

<sup>3</sup>Theory of Polymers and Soft Matter, Department of Applied Physics, Technische Universiteit Eindhoven, 5600 MB Eindhoven, The Netherlands

Correspondence to: A. V. Lyulin (E-mail: a.v.lyulin@tue.nl)

Received 18 October 2013; revised 20 January 2014; accepted 5 February 2014; published online 24 February 2014

DOI: 10.1002/polb.23460

**ABSTRACT:** Revealing the way of how modification of the chemical structure of a polymer affects its macroscopic physical properties offers an opportunity to develop novel polymer materials with pre-defined characteristics. To address this problem two thermoplastic polyimides, ULTEM<sup>TM</sup> and EXTEM<sup>TM</sup>, were simulated with small difference in chemical structures of monomer units, namely, the phenyl ring in ULTEM<sup>TM</sup> was replaced by the diphenylsulphone group in EXTEM<sup>TM</sup>. It is shown that such a small modification results in a drastic difference of the thermal properties: the glass transition temperature of EXTEM<sup>TM</sup> is higher than that of ULTEM<sup>TM</sup>. Our molecular-dynamics simulations clearly demonstrated that it is the electrostatic interactions

that are responsible for the observed difference in thermal properties of ULTEM<sup>TM</sup> and EXTEM<sup>TM</sup>: large partial charges of the sulphone group in the EXTEM<sup>TM</sup> lead to strong dipole–dipole intra- and intermolecular interactions and correspondingly to an elevated glass transition temperature. © 2014 Wiley Periodicals, Inc. *J. Polym. Sci., Part B: Polym. Phys.* **2014**, *52*, 640–646

**KEYWORDS:** computer modeling; EXTEM<sup>TM</sup>; electrostatic interactions; glass transition; molecular dynamics; polyimides; simulations; sulphone group; structure-properties relations; thermal properties; thermoplastics; ULTEM<sup>TM</sup>

**INTRODUCTION** In the last decade polyimides (PI) has become more and more popular as possible constructing materials.<sup>1–3</sup> They found many other industrial applications because of smaller specific weight as compared with, for example, metals, having at the same time comparable toughness and thermal resistance. It is also well known that even minor modifications of a PI chemical structure influences significantly their physical properties and those for PI-based composite materials.<sup>4–8</sup> Nevertheless the existing experimental data are not that predictive in the sense that they cannot unambiguously show which chemical modification influences mainly the properties of the final product. This happens simply because the molecular physical mechanisms which determine the connection of the chemical structure and physical properties are not known at all, or not completely understood in the best case. Such a situation restricts dramatically the possibilities of the synthesis of new thermostable PI with prescribed final-product properties.

In particular, the question remains open how polar groups (i.e., groups with rather large atomic partial charges) influence the PI properties. This is absolutely non-trivial problem,

as the introduction of any group influences not only the distribution of the partial charges along the PI chain backbone, but also its conformational mobility as well. Undoubtedly, computer modeling helps to define better the role and importance of the electrostatic interactions.

Some studies<sup>9–14</sup> deal with molecular-dynamics computer simulations of polymer melts with relatively simple chemical structure and with small partial charges, as for example, polyethylene where partial charges were neglected completely. The absence of the electrostatic terms in the used force fields decreases significantly the required computational resources and, simultaneously, increases the accessible time intervals. This, of course, leads to the acceptable agreement of simulations with existing experiments. Still, the answer remains unknown to which extent such an approach is applicable to PI melts where strongly polarized atoms, or groups of atoms, are definitely present.

In our previous studies<sup>15–19</sup> the atomistic molecular-dynamics simulation has been applied to R-BAPB and R-BAPS PI thermoplastics.<sup>15,20</sup> The chemical structure of these two polymers is

rather similar. The only difference is the presence of the polar sulphone  $\text{SO}_2$  group in the dianhydride part of R-BAPS. The presence of this sulphone group leads to the pronounced difference in the glass transition temperatures ( $T_g$ ) for two polymers, for R-BAPS being 13 K higher as compared with R-BAPB. Our recent computer-simulation results<sup>19</sup> confirm qualitatively this experimental fact. Still, such a difference of only 13 K lies at the upper precision limits of computer simulations,<sup>19</sup> and the question whether the different thermophysical properties of PI R-BAPB and R-BAPS could be explained by different electrostatic interactions or not, remains open.

In the present study the computational investigation has been carried out for two industrial thermoplastics, namely ULTEM<sup>TM</sup> and EXTEM<sup>TM</sup> of SABIC Innovative Plastics.<sup>21–25</sup> The monomer units of these polymers contain the same dianhydride fragments but differ in diamine fragments (Fig. 1). The phenyl ring in the meta position for ULTEM<sup>TM</sup> monomer has been replaced by the diphenylsulphone group in EXTEM<sup>TM</sup>. Such a difference of diamine parts leads to the noticeable difference of the final thermophysical properties of these two polymers, in a very close analogy to R-BAPB and R-BAPS PI discussed above. The largest difference is observed for  $T_g$  values of these PI. For a popular ULTEM<sup>TM</sup> 1000 product in ULTEM<sup>TM</sup> series the value of  $T_g$  is 490 K,<sup>26</sup> for EXTEM<sup>TM</sup> series the  $T_g$  is higher, and is equal to 520 K for EXTEM<sup>TM</sup> VH1003<sup>27</sup> and 540 K for EXTEM<sup>TM</sup> XH1005.<sup>28</sup> Again, we conclude that the PI with strongly polarized sulphone group has higher (by 30–50 K)  $T_g$ .

Computer-simulation methods can be easily implemented for different polymer (in particular, PI) models, with and without partial charges, and undoubtedly can clarify the importance of the electrostatic interactions. In light of the present discussion the agreement between simulations and experiments (i.e., in reproducing the difference between the  $T_g$  for two PI) could be better for PI with electrostatic interactions, only if these electrostatic interactions would be responsible for the observed difference in thermophysical properties. If not, the accounting of electrostatics would not influence the computer simulation results; the values of the  $T_g$  simulated with and without electrostatic interactions would be very close to each other, for each PI. If so, the experimentally observed difference in  $T_g$  should be explained by some other possible physical mechanism, such as chain flexibility or excluded-volume interactions.

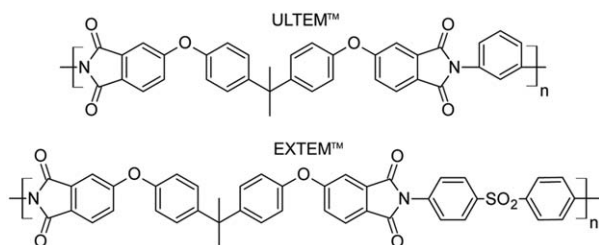


**FIGURE 1** The chemical structures of the repeat units of ULTEM<sup>TM</sup> and EXTEM<sup>TM</sup> PI simulated in the present study.

The rest of this article is organized as follows. The model and the simulation method are described in the section Model and Simulation Method. The details of the equilibration procedure are presented in the section Results and Discussion. The temperature dependence of density for two bulk PI, ULTEM<sup>TM</sup> and EXTEM<sup>TM</sup>, is discussed in the section Results and Discussion in the temperature range from 290 to 600 K. It is shown that the values of the simulated  $T_g$  contradict the experimental data. The  $T_g$ 's calculated from the densities simulated in a broader temperature range, from 290 to 700 K are presented in the section Results and Discussion. The larger temperature range helps to reproduce qualitatively the experimental data provided the electrostatic interactions have been taken into account. Sulphur–sulphur pair correlation functions for EXTEM<sup>TM</sup> model with and without electrostatic interactions are also shown in this section. We argue in this section about the possible molecular mechanism responsible for the changes of the thermophysical properties upon insertion of the polar sulphone group into the PI repeat unit. We finalize the article with conclusions presented as the last section.

## MODEL AND SIMULATION METHOD

Computer simulations of this article have been carried out with Gromacs simulation engine<sup>29,30</sup> using Gromos53a6<sup>31</sup> force field. This force field has been used by us recently for R-BAPB and R-BAPS PI;<sup>16–19</sup> the agreement with experimental data has been obtained in that case. The current simulations have been carried out in NpT ensemble, with three-dimensional (3D) periodic boundary conditions. Temperature and pressure in the simulation box have been controlled by Berendsen thermostat and barostat;<sup>32</sup> the corresponding time constants were taken as 0.1 and 0.5 ps.<sup>16–19</sup> LINCS algorithm<sup>33</sup> has been used to constrain the bond lengths and the integration time step was fixed to 2 fs.

In the present study the computer simulations of the thermostable PI have been carried out with and without electrostatic interactions, the last situation has been achieved by zero atomic partial charges. In general, the partial charges have been calculated as follows.<sup>17</sup> The energy optimization of dimer chemical structures for ULTEM<sup>TM</sup> and EXTEM<sup>TM</sup> has been carried out first. For this purpose Hartree-Fock (HF) method has been used with 6-31G\* basis set of wave functions. Following this optimization, the partial charges have been calculated using the Mulliken method. All quantum-chemical calculations have been performed using Firefly<sup>34</sup> package. The electrostatic interactions have been calculated using PME Ewald summation method.<sup>35,36</sup> For these calculations the cut-off radius in real space was taken as 1 nm, the mesh size for the integration in Fourier space was taken as 0.12 nm.<sup>19</sup> The calculated partial charges for both ULTEM<sup>TM</sup> and EXTEM<sup>TM</sup> will be published soon in our next paper accepted in Polymer Science journal.<sup>37</sup>

The implemented simulation procedure has been already tested in our previous studies.<sup>16–19</sup> It consists of the following stages: (i) creation of the initial non-charged PI

configurations; (ii) compression until the experimental density is reached; (iii) annealing and equilibration; (iv) introduction of partial charges into the corresponding PI model; and, finally, (v) cooling down to room temperature.

The PI initial configurations were produced by random placement of polymer chains in coiled (dumb-bell-like) conformations in a cubic box. The initial volume of the box was chosen big enough to prevent the chains overlap. The cubic cell for each simulated system contains 27 PI chains with polymerization degree  $n = 9$ . For ULTEM™ PI this polymerization degree corresponds to the molecular weights within the “polymer regime”,<sup>38</sup> where the PI  $T_g$  only weakly increases upon the further increase of polymer molecular weight.

After this initialization the stepwise compression was carried out at  $T = 600$  K, namely 1 ns at  $p = 50$  bar, then 2 ns at  $p = 150$  bar, 7 ns at  $p = 300$  bar, 5 ns at  $p = 150$  bar, and finally, 5 ns at  $p = 1$  bar. The total compression time was 20 ns. The compression procedure was followed by the stepwise annealing, with cooling down from  $T = 600$ –290 K and heating up back to 600 K, with the temperature step of 50 K. At each temperature step the system allowed to relax for 2 ns. Such a cooling–heating cycle is repeated three times,<sup>39</sup> afterward the simulation has been performed for another 10 ns at  $T = 600$  K.

The used equilibration procedure of the current study closely follows our previous approach,<sup>16–19</sup> where molecular-dynamics simulation of R-BAPB and R-BAPS PI have been performed, for polymers with similar molecular weight. In our articles<sup>16–19</sup> the quality of the equilibration has been controlled by measuring the average sizes of the individual macromolecules. In equilibrium the chain sizes, first of all, fluctuate around some average values, and, second, are very close to those predicted analytically. The analytical calculations of the individual chain sizes have been carried out using the formalism of virtual bonds.<sup>16,19</sup> About 1.5  $\mu$ s of equilibration has been spent for R-BAPB and R-BAPS at  $T = 600$  K, with zero partial charges. Electrostatic interactions drastically slow down the interchain translational diffusion, and necessary equilibration time is order of magnitude larger. The equilibration of ULTEM™ and EXTEM™ requires some modification of the developed technique<sup>16–19</sup> and will be discussed further in section Results and Discussion.

To study the thermophysical properties of the simulated PI the following approach has been implemented. At the end of the equilibration the 1  $\mu$ s production run has been performed. At every 100 ns the microstate of the system (i.e., the full set of atomic coordinates and atomic velocities) has been dumped, and the cooling down toward room temperature was started. In this way 11 cooling MD trajectories has been obtained. The cooling simulation has been performed stepwise, with  $T = 10$  K step. Three cooling rates were considered; for each rate a step of cooling was followed by 80, 400, or 800 ps annealing at each intermediate temperature. The effective cooling rates of correspondingly  $7.5 \times 10^{12}$  K/min,

$1.5 \times 10^{12}$  K/min, and  $7.5 \times 10^{11}$  K/min are approximately 10–12 orders of magnitude higher than typical experimental values, that are still similar to typical cooling rates of other reported simulations.<sup>40–47</sup> The obtained temperature dependencies of density have been averaged over all 11 systems. For simulated models with electrostatic interactions partial charges have been assigned to atoms of all 11 systems selected during the equilibration with zero partial charges. After this selection the additional equilibration for 100 ns has been carried out, taking into account the full electrostatics, followed by the cooling procedure just described.

The linear fittings were used for low- $T$  (340–410 K) and high- $T$  (650–700 K) domains of the density-temperature curve, and their intersection reveals the simulated  $T_g$ . It should be mentioned that cooling down from 600 to 290 K leads to a coincidence (within statistical error) of the simulated  $T_g$ 's for both PI; and this does not depend on the presence of the atomic partial charges either. Such coincidence contradicts the important  $\Delta T = 30$ –50 K experimental difference between the two  $T_g$ 's. The following explanation of this disagreement is suggested below. A glass transition normally takes place in some temperature range with a width of few tens of K and such region around  $T_g$  should be excluded from the linear fit of density which is used to extract the  $T_g$  value. We can conclude that the temperature interval of 600–290 K is not sufficient in order to measure correctly the  $T_g$ , and should be extended toward higher initial temperature of 700 K. For this reason the polymer melts were heated up from 600 to 700 K with heating rate of  $1.5 \times 10^{12}$  K/min, then the melts were equilibrated at this elevated temperature for 50 ns, and cooling down to 290 K has been started with the cooling rates of  $7.5 \times 10^{12}$  K/min,  $1.5 \times 10^{12}$  K/min, and  $7.5 \times 10^{11}$  K/min. The integration time step was reduced to 1 fs for both heating from 600 to 700 K and cooling from 700 to 290 K, keeping the bonds constrained by LINCS.

## RESULTS AND DISCUSSION

The equilibration procedure consists of few stages. Following our early studies<sup>16–19</sup> 1  $\mu$ s equilibration with integration time step of 2 fs has been carried out at  $T = 600$  K without electrostatic interactions (with zero partial charges). At this stage for each PI the mean-square polymer chain gyration radius  $R_g$  slowly increases (Fig. 2), still remaining below the analytical estimations<sup>16,19</sup> of approximately 3.3 nm and 4.1 nm for ULTEM™ and EXTEM™, respectively. Moreover, at this stage the ULTEM™ chain size exceeds that for EXTEM™ which contradicts theoretical results.

We can roughly conclude that during the initial preparation stage the conformations of the individual PI chains occur to be rather far from Gaussian coils. As for any activated process, the uncoiling of these slightly collapsed conformations requires transitions over some potential energetic barriers. To accelerate these transitions the temperature was increased till  $T = 800$  K and the integration time step was decreased down to 1 fs to keep the simulations stable. At this (and only at this) stage we had also switched off the LINCS algorithm which

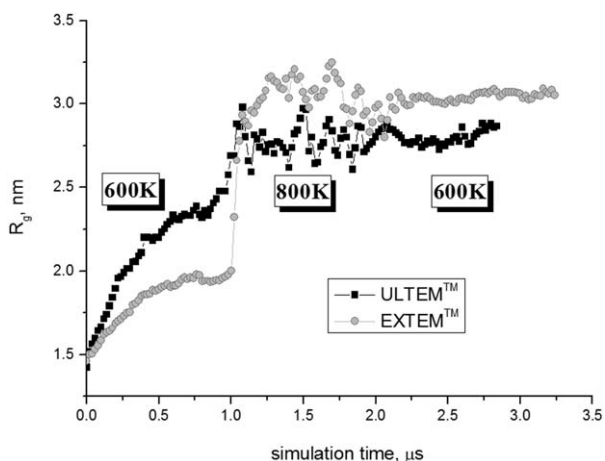


**FIGURE 2** Time dependence of the chain mean-square gyration radius for bulk ULTEM™ and EXTEM™ PI. Each point has been obtained by averaging over all polymer chains during 20 ns of simulation. The number inside the figure indicates the temperature at equilibration stages. Stages at  $T = 600$  K were implemented with integration step of 2 fs, with LINCS-constrained bonds. Stages at  $T = 800$  K were performed with the integration step of 1 fs, without LINCS-constrained bonds.

keeps the covalent bonds constant. Due to the equilibration carried out in this regime for 1  $\mu$ s the individual chain dimensions increase significantly (Fig. 2). Finally, the temperature was decreased down to  $T = 600$  K, the integration time step was returned back to 2 fs, and LINCS algorithm was switched on. This last equilibration stage is carried out for one more microsecond; during this stage the chain sizes do not change and fluctuate around some average values of approximately 2.8 and 3.0 nm for ULTEM™ and EXTEM™, respectively. Note that the gyration radius for EXTEM™ chain is approximately 8% larger than the corresponding value for ULTEM™, supporting qualitatively the analytical calculations. The average values of  $R_g$  and the end-to-end distance do not change notably after introducing the partial atomic charges.

The cooling of both PI models (with and without partial charges) has been carried out following the algorithm described in section Model and Simulation Method. The simulated  $T$ -dependencies of the corresponding densities are shown in Figure 3. These dependencies were linearly fitted using two temperature intervals, 340–410 K and 650–700 K. From the intersections of the low-temperature fittings for all cooling rates with high-temperature fitting for the slowest cooling rate the values of the glass transition temperature, Table 1, were calculated.

The analysis of the data in Table 1 shows that our simulations demonstrate a correct cooling rate dependence of  $T_g$ : it decreases with decrease in cooling rate (in the case of ULTEM™ with partial charges,  $T_g$  value remains the same within an error of several Kelvins). Besides this all simulated values of  $T_g$  (either with or without partial charges)

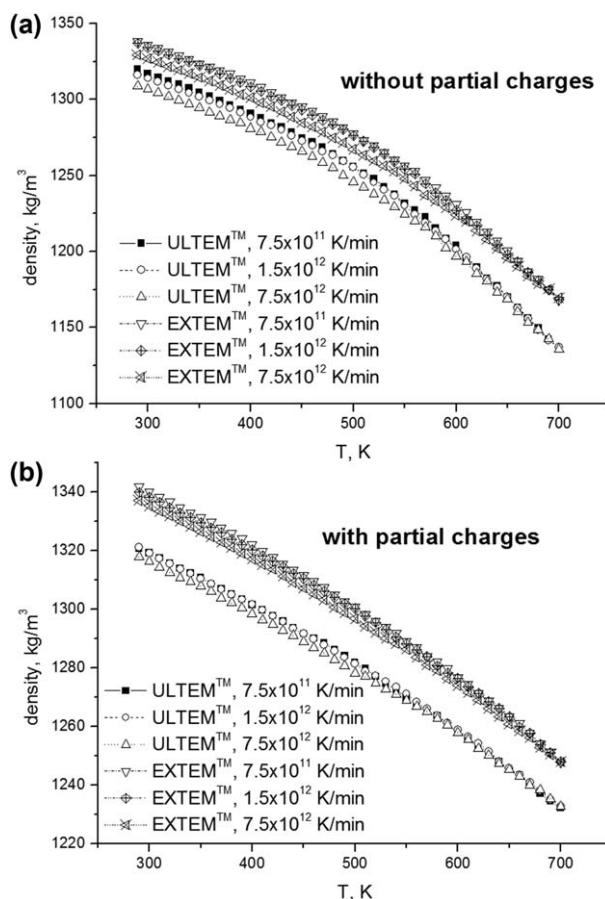


**FIGURE 3** Simulated temperature dependence of ULTEM™ and EXTEM™ density, for models (a) without and (b) with partial charges, obtained by cooling the melts down from 700 to 290 K.

are above or at least not less than the corresponding experimental results ( $T_g^{\text{ULTEM}} = 490$  K;  $T_g^{\text{EXTEM}} = 520 - 540$  K).<sup>25</sup> Besides this the values of  $T_g$  obtained from the simulations with partial charges are higher than those without partial charges for the same systems due to enhanced rigidity caused by electrostatic interactions.

The change of  $T_g$  value is higher for EXTEM™ than for ULTEM™ with partial charges for all the values of cooling rate considered. We conclude that, in spite of the presence of charge polar groups in both PI (in heterocycles, or in

**TABLE 1** Simulated Values of the Glass Transition Temperature for Both PI

Cooling Rate	$7.5 \times 10^{12}$ K/min	$1.5 \times 10^{12}$ K/min	$7.5 \times 10^{11}$ K/min
$T_g^{\text{ULTEM}}^{\text{TM}}$	539/552	525/536	523/544
$T_g^{\text{EXTEM}}^{\text{TM}}$	561/597	544/575	524/556
$\Delta T_g$	22/45	19/39	1/12

The values of  $T_g$  for the systems without/with partial charges are given with a slash.  $\Delta T_g = T_g^{\text{EXTEM}} - T_g^{\text{ULTEM}}$ .



ether bridges) the influence of the sulphone group is much higher, and is mainly responsible for the different thermophysical properties of these two polymers. Note that in our recent studies the similar effect was observed for R-BAPS PI which, as in the case of EXTEM<sup>TM</sup>, contains highly polar sulphone group. For R-BAPS model melt the  $T_g$  values were much higher when electrostatic interactions (and partial charges of sulphone group) have been taken into account.

It should also be noted that with full electrostatics the simulated EXTEM<sup>TM</sup>  $T_g$  is well above that for ULTEM<sup>TM</sup>. Exactly this difference is shown in experiment. We conclude that, again, it is electrostatics which is mainly responsible for much higher glass transition temperature for EXTEM<sup>TM</sup> PI.

The computer simulations of the glass transitions in two PI reveal the results which agree qualitatively with the existing experiments. Nevertheless this agreement should be further confirmed; the  $T_g$  value depends on the cooling rate, and no one can guarantee that this cooling-rate dependence is the same for different PI. The coefficient of polymer thermal expansion (CTE) represents more universal characteristic which does not depend on the cooling rate. In the present study the CTE has been calculated using the temperature dependencies of density shown in Figure 3. As in experiment, the temperature interval from 300 to 430 K has been used for these calculations. The data in Table 2 shows that the simulated CTE values are very close to the experimental results. They do not depend on the magnitude of the simulated cooling rate, in agreement with our previous simulations.<sup>18</sup>

In addition, we can conclude that the electrostatic interactions in the EXTEM<sup>TM</sup> model lead to much better agreement between simulated and experimental values of CTE.

Density is another physical characteristic which can be used to compare simulations and experiments. The known experimental values of density at room temperature are 1270 kg/m<sup>3</sup> for ULTEM<sup>TM</sup> and 1300 kg/m<sup>3</sup> for EXTEM<sup>TM</sup>,<sup>26–28</sup> the corresponding simulated values at  $T = 290$  K are 1320 kg/m<sup>3</sup> for ULTEM<sup>TM</sup> and 1340 kg/m<sup>3</sup> for EXTEM<sup>TM</sup> (Fig. 3). The simulations give slightly higher values for both PI, the ULTEM<sup>TM</sup> density is about 20 kg/m<sup>3</sup> lower, which is also in agreement with experiment. The density is slightly higher for models with partial charges and electrostatic interactions due to some structural rearrangements caused by dipole–dipole interactions. The den-

**TABLE 2** Coefficients of Thermal Expansions Simulated by Cooling the PI Down from 700 K, and Measured in a Temperature Range 300–430 K

	Without Partial Charges, 10 <sup>-4</sup> 1/K	With Partial Charges, 10 <sup>-4</sup> 1/K	Experiments, 10 <sup>-4</sup> 1/K
ULTEM <sup>TM</sup>	2.0	1.4	1.7 <sup>24</sup>
EXTEM <sup>TM</sup>	2.0	1.4	1.5 <sup>25</sup>

sity curves for the same system obtained upon cooling with lower rate are above those obtained with higher rate, demonstrating an expected behavior.

It was shown earlier that the electrostatic interactions strongly influence the thermophysical properties of EXTEM<sup>TM</sup>, and are of less importance for ULTEM<sup>TM</sup>. The only difference in chemical structure of two PI is the existence of strongly polarized sulphone group in EXTEM<sup>TM</sup> monomer unit. We suggest that the structural changes due to the presence of this group are mainly responsible for different thermophysical characteristics. As suggested in ref. 20, the sulphur–sulphur pair correlation function has been calculated in the present study at  $T = 700$  K for EXTEM<sup>TM</sup>, in order to check these structural changes (Fig. 4).

It is clearly seen that at small distances, below 1.5 nm, the electrostatic interactions lead to few maxima in this function. These picks reflect some local structuring of sulphone groups. Earlier it was reported that some clustering of sulphone groups is taking place if the partial charges are calculated by AM1 method.<sup>19</sup> Most probably the clustering of sulphone groups is not present here, otherwise the strong (and the only) first maximum at very small distances should be observed in Figure 4.

At the same time pair radial distribution functions for carbon atoms of aromatic rings are very similar for both systems, with and without partial charges (Fig. 5). Two well-recognized peaks may correspond to the formation of intermolecular contacts between aromatic rings due to  $\pi$ -stacking.

## CONCLUSIONS

The presented computer simulations of two thermostable PI, ULTEM<sup>TM</sup> and EXTEM<sup>TM</sup>, reproduce qualitatively the higher value of  $T_g$  for EXTEM<sup>TM</sup>, confirming the existing experimental data. It was shown that this agreement can be reached only by taking into account two factors. First of all, the simulated temperature range should be broadened, and the cooling down

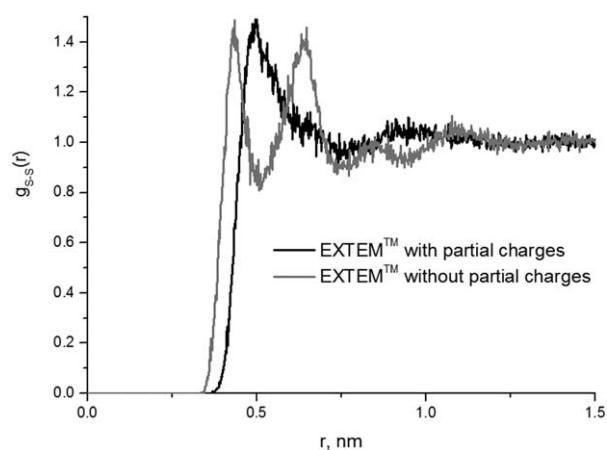


**FIGURE 4** Pair radial distribution function  $g_{S-S}(r)$  of sulphur atoms located at a given distance  $r$  from each other for bulk EXTEM<sup>TM</sup> at  $T = 700$  K.

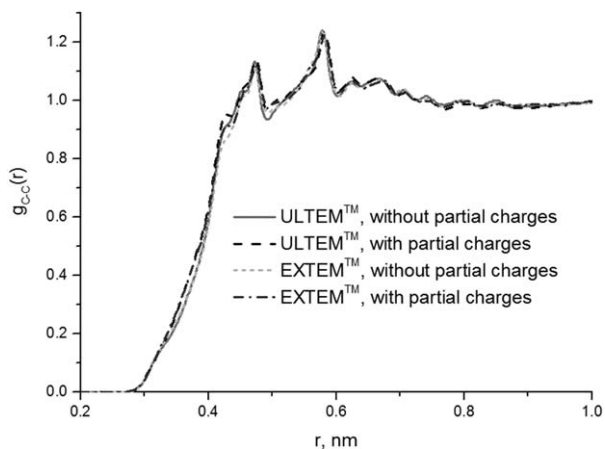


**FIGURE 5** Pair radial distribution function  $g_{C-C}(r)$  of aromatic ring carbon atoms located at a given distance  $r$  from each other.

should be started from higher temperatures. This allows using the linear fit of  $T$ -dependence of density exploring larger temperature intervals, and excluding the glass-transition zone with strong non-linear density  $T$ -dependence. In the present simulations the initial PI melt temperature was shifted from  $T = 600$  to  $700$  K, and the cooling stops at  $T = 290$  K. We have also shown that the presence of the electrostatic interactions lead to much better agreement with existing experimental data. It is electrostatic interactions which finally responsible for the changes in thermophysical properties of PI upon the modification of their chemical structure by introducing the polar groups. The accompanying changes of flexibility and specific volume influence the thermophysical properties much weaker. As a consequence of strong electrostatic interactions between polar groups, some local structural ordering of PI fragments takes place.

#### ACKNOWLEDGMENTS

This study has been supported by the Russian Ministry of Education and Science within State Contract No. 14.Z50.31.0002 (megagrant of the Government of the Russian Federation according to the Resolution No. 220 of April 9, 2010). All computer simulations have been carried out using the computational facilities of the Institute of Macromolecular Compounds, Russian Academy of Sciences, and supercomputers “Chebyshev” and “Lomonosov” of the Lomonosov Moscow State University.

#### REFERENCES AND NOTES

- 1 A. Baker, S. Dutton, D. Kelly, Composite materials for aircraft structures, 2nd ed.; American Institute of Aeronautics and Astronautics: Reston, Virginia, **2004**.
- 2 A. P. Mouritz, A. G. Gibson, Fire properties of polymer composite materials; Springer: Dordrecht, **2006**.
- 3 D. Gay, S. V. Hoa, S. W. Tsai, Composite materials. Design and application; CRC Press: London, **2003**.

- 4 X.-Y. Wang, P. J. in 't Veld, Y. Lu, B. D. Freeman, I. C. Sanchez, *Polymer* **2005**, *46*, 9155–9161.
- 5 J. Xia, S. Liu, P. K. Pallathadka, M. L. Chng, T. S. Chung, *Ind. Eng. Chem. Res.* **2010**, *49*, 12014–12021.
- 6 M. I. Bessonov, M. M. Koton, V. V. Kudryavtsev, L. A. Laius, Polyimides—thermally stable polymers; Consultants Bureau: New York, **1987**.
- 7 V. L. Bell, B. L. Stump, H. Gager, *J. Polym. Sci., Polym. Chem. Ed.* **1976**, *14*, 2275–2291.
- 8 C. E. Sroog, *Prog. Polym. Sci.* **1991**, *16*, 561–694.
- 9 A. V. Lyulin, N. K. Balabaev, M. A. J. Michels, *Macromolecules* **2003**, *36*, 8574–8575.
- 10 R. Bruning, K. Samwer, *Phys. Rev. B* **1992**, *46*, 11318–11322.
- 11 K. Vollmayr, W. Kob, K. J. Binder, *J. Chem. Phys.* **1996**, *105*, 4714–4728.
- 12 J. J. Baschnagel, *J. Phys: Condens. Matter.* **1993**, *5*, 1597–1618.
- 13 A. V. Lyulin, M. A. J. Michels, *Macromolecules* **2002**, *35*, 9595–9604.
- 14 D. Hudzinskyy, A. V. Lyulin, A. R. C. Baljon, N. K. Balabaev, M. A. J. Michels, *Macromolecules*, **2011**, *44*, 2299–2310.
- 15 V. E. Yudin, V. M. Svetlichnyi, *Russ. J. Gen. Chem.* **2010**, *80*, 2157–2169.
- 16 V. M. Nazarychev, S. V. Larin, N. V. Lukasheva, A. D. Glova, S. V. Lyulin, *Polym. Sci. Ser. A* **2013**, *55*, 570–576.
- 17 S. V. Lyulin, A. A. Gurtovenko, S. V. Larin, V. M. Nazarychev, A. V. Lyulin, *Macromolecules* **2013**, *46*, 6357–6363.
- 18 S. V. Lyulin, S. V. Larin, A. A. Gurtovenko, V. M. Nazarychev, S. G. Falkovich, V. E. Yudin, V. M. Svetlichnyi, I. V. Gofman, A. V. Lyulin, *Soft Matter* **2014**, *10*, 1224–1232.
- 19 S. V. Lyulin, S. V. Larin, A. A. Gurtovenko, N. V. Lukasheva, V. E. Yudin, V. M. Svetlichnyj, A. V. Lyulin, *Polym. Sci. Ser. A* **2012**, *54*, 631–643.
- 20 V. E. Yudin, G. M. Divoux, J. U. Otaigbe, V. M. Svetlichnyi, *Polymer* **2005**, *46*, 10866–10872.
- 21 Y. Wang, L. Y. Jiang, T. Matsuurac, T. S. Chung, S. H. Goh, *J. Membr. Sci.* **2008**, *318*, 217–226.
- 22 N. Peng, T. S. Chung, M. L. Chung, W. J. Aw, *J. Membr. Sci.* **2010**, *360*, 48–57.
- 23 J. Xia, S. Liu, P. K. Pallathadka, M. L. Chng, T. Chung, *Ind. Eng. Chem. Res.* **2010**, *49*, 12014–12021.
- 24 ULTEM™ [Online], <http://www.sabic-ip.com/gep/en/ProductsAndServices/SpecialtyAdditivesandIntermediatesProductPages/ultempesinsadditives.html>
- 25 EXTEM™ [Online], <http://www.sabic-ip.com/gep/en/ProductsAndServices/SpecialtyAdditivesandIntermediatesProductPages/extemthermoplasticpolyimideresins.html>
- 26 ULTEM™ 1000 [Online], <http://kbam.geampod.com/KBAM/Reflection/Assets/20326.pdf>
- 27 EXTEM™ VH1003 [Online], <http://kbam.geampod.com/KBAM/Reflection/Assets/20311.pdf>
- 28 EXTEM™ XH1005 [Online], <http://kbam.geampod.com/KBAM/Reflection/Assets/20312.pdf>
- 29 B. Hess, C. Kutzner, D. van der Spoel, E. J. Lindahl, *J. Chem. Theory Comput.* **2008**, *4*, 435–447.
- 30 D. van der Spoel, E. Lindahl, B. Hess, G. Groenhoff, A. E. Mark, H. J. C. Berendsen, *J. Comput. Chem.* **2005**, *26*, 1701–1718.
- 31 C. Oostenbrink, A. Villa, A. E. Mark, W. F. van Gunsteren, *J. Comput. Chem.* **2004**, *25*, 1656–1676.

- 32** H. J. C. Berendsen, *Computer simulations in materials science*; Kluwer: Dordrecht, **1991**.
- 33** B. Hess, H. Bekker, H. J. C. Berendsen, J. G. E. M. Fraaije, *J. Comput. Chem.* **1997**, *18*, 1463–1472.
- 34** A. A. Granovsky, Firefly version 7.1.G, [Online], <http://classic.chem.msu.su/gran/firefly/index.html>.
- 35** T. Darden, D. York, L. Pedersen, *J. Chem. Phys.* **1993**, *98*, 10089–10092.
- 36** U. Essmann, L. Perera, M. L. Berkowitz, T. Darden, H. Lee, L. G. Pedersen, *J. Chem. Phys.* **1995**, *103*, 8577–8593.
- 37** S. G. Falkovich, S. V. Larin, V. M. Nazarychev, I. V. Volgin, A. A. Gurtovenko, A. V. Lyulin, S. V. Lyulin, *Polym. Sci. Ser. A* **2014**, in press.
- 38** J. V. Facinelli, S. L. Gardner, L. Dong, C. L. Sensenich, R. M. Davis, J. S. Riffle, *Macromolecules* **1996**, *29*, 7342–7350.
- 39** P. V. Komarov, Y.-T. Chiu, S.-M. Chen, P. Reineker, *Macromol. Theory Simul.* **2010**, *19*, 64–73.
- 40** Y. Chen, Q. L. Liu, A. M. Zhu, Q. G. Zhang, J. Y. Wu, *J. Membr. Sci.* **2010**, *348*, 204–212.
- 41** S. Velioglu, M. G. Ahunbay, S. B. Tantekin-Ersolmaz, *J. Membr. Sci.* **2012**, 417–418, 217–227.
- 42** M. Minellia, M. G. De Angelisa, D. Hofmann, *Fluid Phase Equilibria* **2012**, *333*, 87–96.
- 43** L. Zhang, Y. Xiao, T.-S. Chung, J. Jiang, *Polymer* **2010**, *51*, 4439–4447.
- 44** Y. Yani, M. H. Lamm, *Polymer* **2009**, *50*, 1324–675.
- 45** M. Li, X. Y. Liu, J. Q. Qin, Y. Gu, *Express Polym. Lett.* **2009**, *3*, 665–675.
- 46** A. Soldera, N. Metatla, *Phys. Rev. E* **2006**, *74*, 061803.
- 47** D. Qi, J. Hinkley, G. He, *Model. Simul. Mater. Sci. Eng.* **2005**, *13*, 493–507.